Feature-Based Medical Image Registration using a Fuzzy Clustering Segmentation Approach

Hassan Mahmoud, Francesco Masulli*, and Stefano Rovetta

Dipartimento di Informatica, Bioingegneria, Robotica e Ingegneria dei Sistemi, Università di Genova, and CNISM Genova Research Unit, Via Dodecaneso 35, I-16146 Genova, Italy
* Center for Biotechnology, Temple University, Philadelphia, USA
{hassan.mahmoud|francesco.masulli|stefano.rovetta}@unige.it

Abstract. This paper presents an approach to medical image registration using a segmentation step segmentation based on Fuzzy C-Means (*FCM*) clustering and the Scale Invariant Feature Transform (*SIFT*) for matching keypoints in segmented regions. To obtain robust segmentation, FCM is applied on feature vectors composed by local information invariant to image scaling and rotation, and to change in illumination. *SIFT* is then applied to corresponding regions in reference and target images, after the application of an $alpha$-cut. The proposed registration method is more robust to noise artifacts than standard *SIFT*. The paper shows also a method for *FCM* clustering speeding-up based on a dynamic pyramid approach using low resolution images of increasing size.

1 Introduction

Image registration [13] is the process of aligning images so that corresponding features can easily be related. In medical imaging it allows us to extract complementary information from different modalities, and to compare accurately images from the same modality [4,10]. Recently, registration has been also applied in image guided surgery interventions, and in serial imaging analysis for the study of diseases progression.

To achieve image registration, the computer rotates, scales and translates one image (*target image*) to match another image (*reference image*). Methods to perform the registration can be categorized as feature-based, intensity-based, and gradient-based, although hybrid approaches are possible [13]. In feature-based methods the registration is based on the correspondence of a small set of salient points, landmarks, or on alignment of segmented binary structures in images being registered (e.g., lines, curves or points matching). These methods are relatively fast, but they are lacking in robustness of feature extraction and accuracy of feature matching. Furthermore, extracted features need to be invariant to image deformations. To this aim, because of the noise entailed in medical images, some preprocessing steps are usually applied to enhance feature appearance using image gradients and gamma corrections. In particular, the accuracy of the registration result depends on the quality of the previous region segmentation procedure.

Medical image segmentation methods are usually based on gray level features (e.g., histograms, edges, regions), texture features (e.g., first or higher order statistics, spectral methods) correspondence, or also on model based or atlas based techniques [13,14].

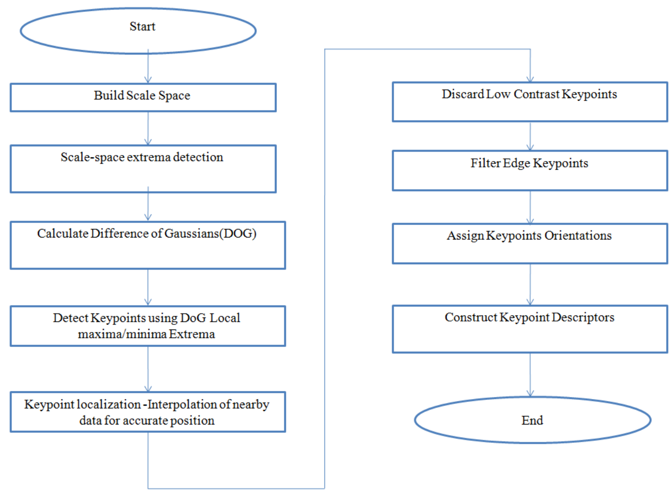

Fig. 1. *SIFT* feature detection technique.

Recently, artificial neural network methods and clustering techniques have been successfully applied [11,9].

In this paper we apply fuzzy clustering to automatically detect robust candidate regions for a registration method based on the Scale Invariant Feature Transform (*SIFT*) [6] that is a popular feature-based image registration method matching points using a similarity measure.

This paper is organized as follows: The Scale Invariant Feature Transform and Fuzzy C-Means clustering algorithm are presented in Sect.s 2 and 3; Sect. 4 presents the proposed *FCM–SIFT* registration framework; results and discussion are in Sect. 5; Sect. 6 contains the conclusions.

2 Scale Invariant Feature Transform

In Scale-Invariant Feature Transform (*SIFT*) [6], robust and salient reference points (keypoints) of objects are extracted from reference image and from a target image to be co-registered respect to it. Fig. 1 shows our implementation of *SIFT* to detect keypoints from corresponding segmented regions in the reference and target images. The main steps are:

1. *Scale-space extrema detection*. In this step we search over all scales and image locations by using a Difference-of-Gaussian function (DoG) to identify potential interest points that are invariant to scale and orientation. We compare each pixel in the DoG images to its eight neighbors at the same scale and nine corresponding neighboring pixels in each of the neighboring scales. If the pixel value is the maximum or minimum among all compared pixels, it is selected as a candidate

key-point. Specifically, a DoG image $D(x, y, \sigma)$ is given by:

$$D(x, y, \sigma) = L(x, y, k_i\sigma) - L(x, y, k_j\sigma), \tag{1}$$

where $L(x, y, k\sigma)$ is the convolution of the original image $I(x, y)$ with the Gaussian kernel

$$G(x, y, \sigma) = \frac{1}{2\pi\sigma^2} e^{-\frac{x^2+y^2}{2\sigma^2}} \tag{2}$$

at scale $k\sigma$, i.e.,

$$L(x, y, k\sigma) = G(x, y, k\sigma) * I(x, y) \tag{3}$$

Note that this first step produces many keypoints.

2. *Key-point localization*. keypoints are selected using measures of their stability, using nearby data, scale, and ratio of principal curvatures. This information allows points to be rejected that have low contrast and are sensitive to noise or poorly localized along an edge.
3. *Orientation assignment*. Orientations are then assigned on the basis of local image gradient directions to each key-point for rotation invariance. *SIFT* operates on data transformed to the assigned orientation, scale, and location for each feature, providing invariance to these transformations. For an image sample $L(x, y)$ at scale σ, the gradient magnitude, $m(x, y)$, and orientation $\Theta(x, y)$, are pre-computed using pixel differences:

$$m(x, y) = \sqrt{[(L(x+1, y, \sigma) - L(x-1, y, \sigma)]^2 + [(L(x, y+1, \sigma) - L(x, y-1, \sigma)]^2} \tag{4}$$

and

$$\Theta(x, y) = tan^{-1}\left(\frac{L(x+1, y, \sigma) - L(x-1, y, \sigma)}{L(x, y+1, \sigma) - L(x, y-1, \sigma)}\right) \tag{5}$$

where $L(x, y, \sigma)$m is the Gaussian smoothed image.

After applying *SIFT* on target and reference images we obtain the set of salient feature points. It is worth noting that the quality of *SIFT* results, as for other feature-based methods for registration, is strongly affected by the quality of the previous region segmentation procedure.

3 Fuzzy C-Means Algorithm

The determination of consistent clusters, i.e., matched segments/regions in the reference and target images is a main step in *SIFT*. In [6], clustering is performed by the generalized Hough transform. In the approach we propose in this paper clustering is obtained using the Fuzzy C-Means [1] (*FCM*) clustering algorithm.

The *FCM* algorithm is aimed to the minimization of the following functional:

$$J_m(\mathbf{U}, Y) \equiv \sum_{i=1}^{n} \sum_{k=1}^{c} (u_{ik})^m E_k(x_i) \tag{6}$$

where: $X = \{x_1, x_2, \ldots, x_n\}$ is a data set containing n unlabeled sample points; $Y = \{y_1, y_2, \ldots, y_c\}$ is the set of the centers of clusters; $\mathbf{U} = [u_{ik}]$ is the $c \times n$ fuzzy c-partition matrix, containing the membership values of all samples to all $m \in (1, \infty)$ is the fuzziness control parameter; $E_k(x_i)$ is a dissimilarity measure (distance or cost) between data point x_i and the center y_k of a specific cluster k. We use the Euclidean distance $E_k(x_i) = \|x_i - y_k\|^2$ as the dissimilarity measure.

The clustering problem can be formulated as the minimization of J_m with respect to Y, under the normalization constraint $\sum_{k=1}^{c} u_{ik} = 1$.

The necessary conditions for minimization of J_m are then:

$$y_k = \frac{\sum_{i=1}^{n} (u_{ik})^m x_i}{\sum_{i=1}^{n} (u_{ik})^m} \qquad \text{for all } k, \tag{7}$$

$$u_{ik} = \begin{cases} \left(\sum_{l=1}^{c} \frac{E_k(x_i)}{E_l(x_i)} \right)^{\frac{2}{1-m}} & \text{if } \; E_k(x_i) > 0 \; \forall k, i; \\ 1 \quad \text{if } \; E_k(x_i) = 0 \quad \text{and} \quad u_{il} = 0 \;\; \forall \, l \neq k & \end{cases} \tag{8}$$

The Fuzzy C-Means algorithm starts with a random initialization of the fuzzy c-partition matrix $\mathbf{U}$ (or of the centroids y_k) and then implements a Picard iteration of Eq.s 7 and 8 until convergence (defined, e.g., as when the change of centroids is smaller than an assigned threshold).

Note that if one chooses $m = 1$ the Fuzzy C-Means functional J_m (Eq. (6)) reduces to the expectation of the K-Means (*KM*) global error $< E > \equiv \sum_{i=1}^{n} \sum_{k=1}^{c} u_{ik} E_k(x_i)$, and the *FCM* becomes the crisp *KM* algorithm [15,5,3].

4 Fuzzy C-Means based Scale Invariant Feature Transform

As already stated, in our proposed approach for image registration *SIFT* operates on the matched segments (clusters) obtained from *FCM*. Starting from those segments, *SIFT* extracts the matching keypoints in both reference and target images and obtains the registration parameters able to recover their correspondence.

In order to find robust and reliable clusters, *FCM* must be performed in a feature space with features invariant to image scaling and rotation. In our approach, for each pixel we consider intensity value, spatial location, and neighborhood average intensity and deviation from the eight surrounding pixels. These features are well localized in both the spatial and frequency domains (reducing the probability of disruption by occlusion, clutter, or noise), are invariant to image scaling and rotation, and are partially invariant to moderate changes in illumination and 3D camera viewpoint [2,12,7].

After clustering the two images, we select the minimal volume (fuzzy cardinality) cluster, corresponding to a region in each image, and then we apply an α-cut, where α is a threshold selected in the interval $[0, 1]$ that selects pixels with high membership to cluster. This approach minimizes the search space for finding the correspondence of keypoints, as it selects the most reliable pixels of the region. Note that, if $\alpha = 0$ we get the whole pixels of the segmented region, while if $\alpha = 1$ we select pixels having stronger membership to the cluster only, but this sub-set could be empty or could lose

Table 1. The *FCM–SIFT* registration framework.

1. *Image Preprocessing*: Adjust threshold gray level enhancement in both target and reference images and obtain image pyramid.
2. *Segment Extraction*: Apply *FCM* on target and reference images with c clusters and obtain **U** fuzzy membership matrix.
3. *Segment matching*:
   (a) Calculate cluster volumes from the fuzzy membership matrix **U**.
   (b) Find the minimum volume clusters in both images (which represent the smallest matched region in the two images) and and extract two reliable segments from them withan α-cut.
4. *Feature matching*: Apply *SIFT* on both segments to extract invariant robust feature points.
5. *Registration*:
   (a) Infer spatial correspondence between at least two points of extracted matched feature points in both images.
   (b) Extract registration parameters.
   (c) Apply spatial transformation on target image.

Table 2. Experiments. For each experiment we report: horizontal translation (Tx), vertical translation (Ty), rotation degree (R), and scaling factor (S).

Experiment	Tx	Ty	R	S
T1	20	20	252	1.0
T2	-30	-30	0	.6
T3	40	0	324	1.3
T4	0	-10	144	.8
T5	-20	-20	120	.7

good key-point candidates. Therefore, we choose the highest value of α that select a region with a size corresponding to an assigned percentage of the full image.

The steps of the proposed *FCM–SIFT* registration framework are described in Tab. 1. At the end of the *FCM–SIFT* registration, we obtain the registration parameters between target and reference images (namely, horizontal translation Tx, vertical translation Ty, rotation angle R, and scaling factor S).

5 Experimental Results and Discussion

We validated our *FCM–SIFT* registration framework on a sample set of Computer Tomography (CT) images of the head. The software was developed in Matlab R2009b under Windows 7 32 bit. The computation time ($Time$) was evaluated on a laptop with 2.00 GHz dual-core processor and 3.25 GB of RAM. As usual, time is given as a rough indication only, with the additional caveat that Matlab is inefficient in specific operations, for instance loops.

The target images where obtained by transforming the original image with a combination of translation, rotation, and anisotropic scaling.

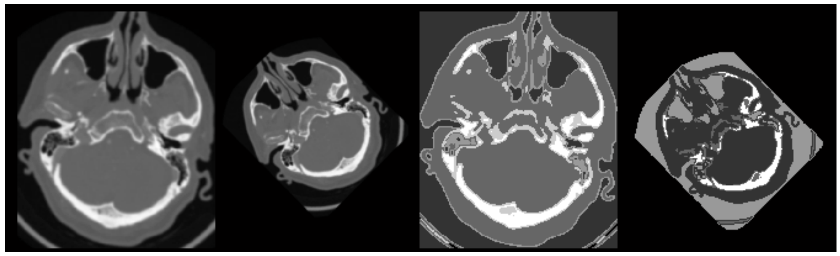

(a)

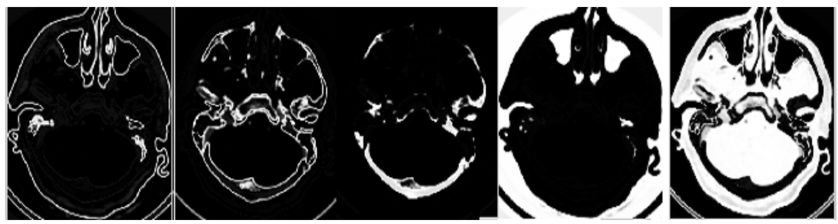

(b)

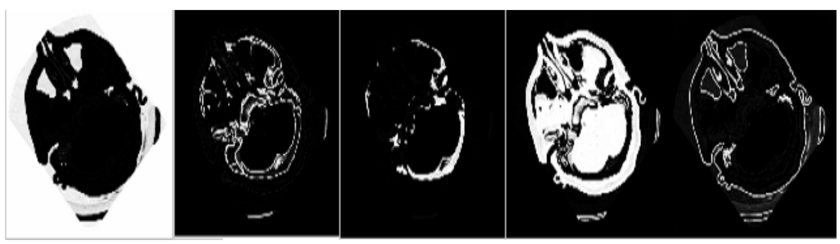

(c)

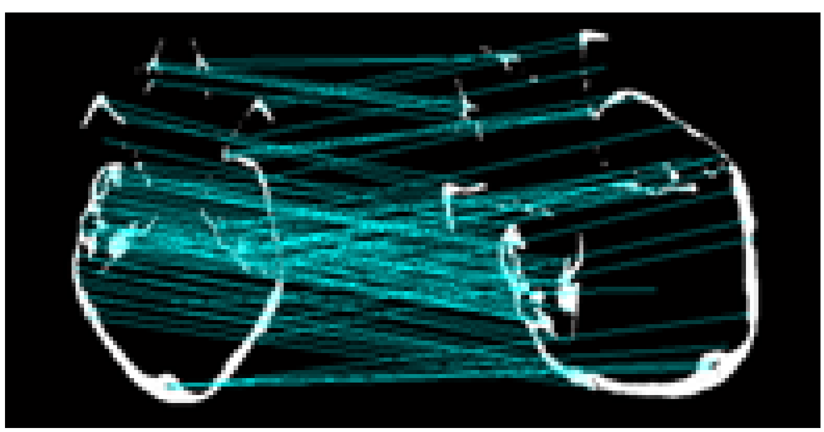

(d)

Fig. 2. Axial CT head plane. (a) From left to right: Reference image, target image, segmented reference image, and segmented target image. (b) The five clusters obtained from the reference image. (c) The five clusters obtained from the target image. (d) *SIFT* matching using the minimal volume regions, after α-cut.

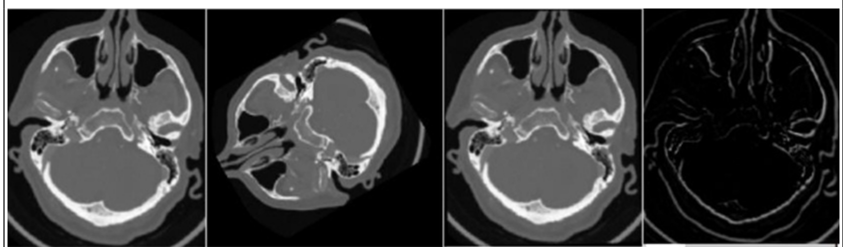

Axial plane: $Tx = -1$, $Ty = 3$, $R = -1.7$, $S = 0.00$,
$Time = 18$, $CC = 0.84$, $MSE = 31.80$

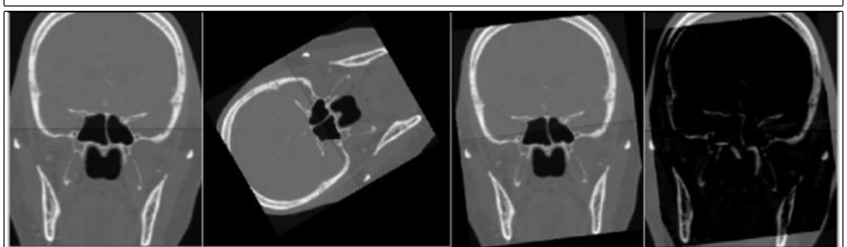

Coronal plane: $Tx = 0$, $Ty = 0$, $R = -2.73$, $S = 0.06$,
$Time = 52$, $CC = 0.68$, $MSE = 35.74$

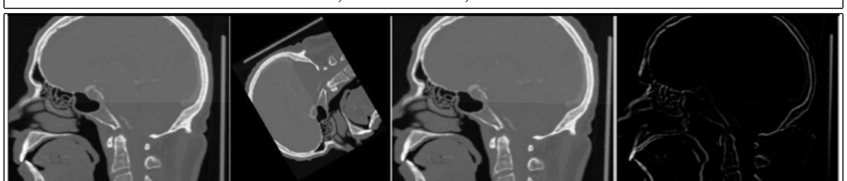

Sagittal plane: $Tx = -1$, $Ty = -1$, $R = -0.15$, $S = 0.00$
$Time = 24$, $CC = 0.99$, $MSE = 7.54$

Fig. 3. *FCM–SIFT* registration results with CT of head on axial, sagittal, and coronal planes. From left to right: reference, moving, registered, and error images.

Fig. 2 shows the segment extraction on axial head CT slice on reference and target images using *FCM* clustering. In Fig. 2a, from left to right, there are the reference image, the target image, the segmented reference image, and the segmented target image. *FCM* is performed using a number of clusters $c = 5$ estimated on the basis of a-priori experimental knowledge and a fuzzyfication parameter $m = 2$. Fig.s 2b and 2c show the five clusters obtained from reference and target images. After clustering, we identified in the two images the segments with minimal volumes to be matched. Then we selected the regions with points with highest memberships by applying the α-cut thresholding. Finally, we applied the *SIFT* on this pair of sub-regions. Fig. 2d shows *SIFT* matching of salient keypoints of the selected regions.

Fig. 3 illustrates some *FCM–SIFT* registration results with CT on axial, sagittal, and coronal planes. For each projection, we report, from left to right, the reference and target

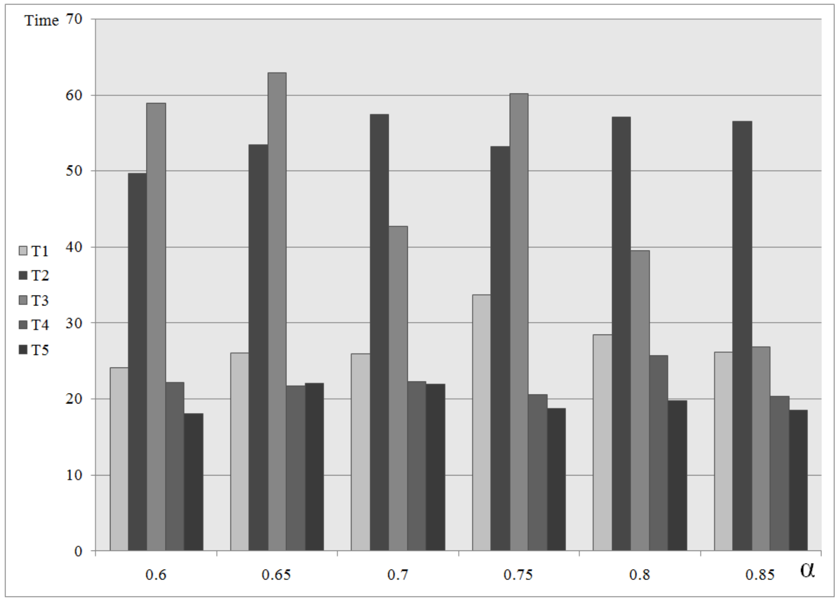

(a)

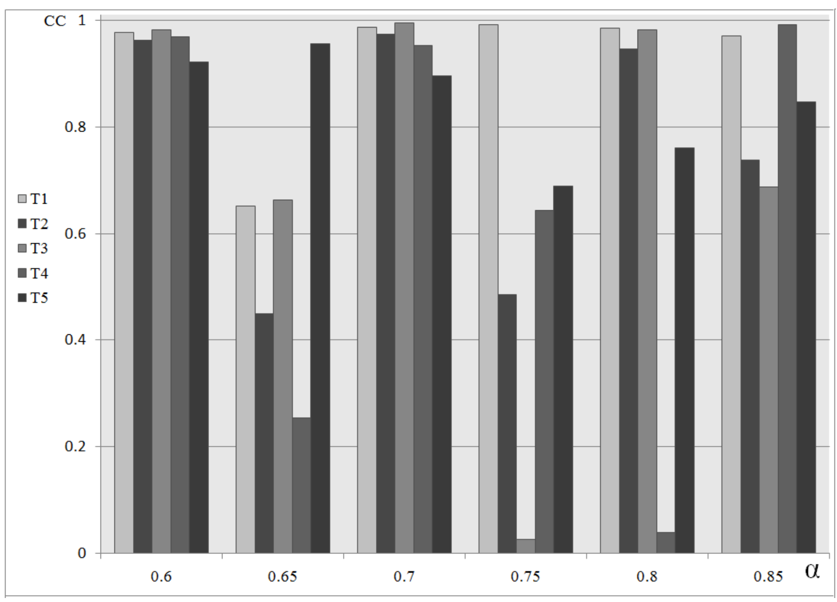

(b)

Fig. 4. Experiments T1–T5: Running time in seconds (a) and cross correlation between registered and reference images (b) v.s. threshold α.

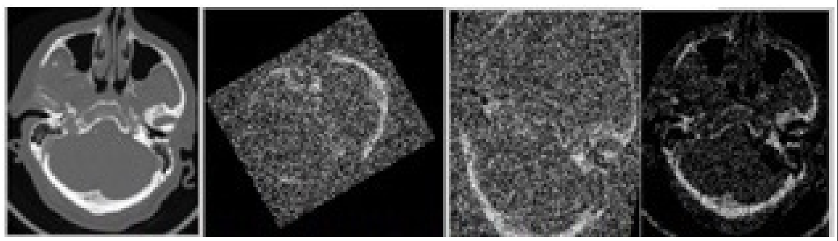

Axial plane: $Tx = 7$, $Ty = 7$, $R = 13.78$, $S = 0.43$,
$Time = 84$, $CC = 0.05$, $MSE = 72.86$

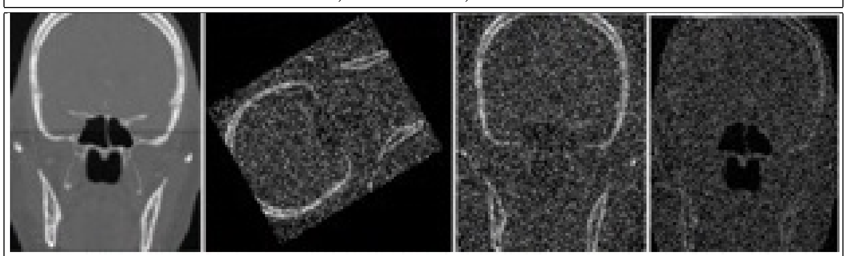

Coronal plane: $Tx = 0$, $Ty = 1$, $R = 0.44$, $S = 0.00$,
$Time = 54$, $CC = 0.42$, $MSE = 59.20$

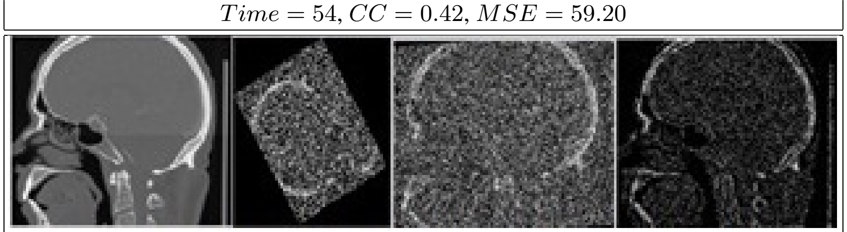

Sagittal plane: $Tx = 1$, $Ty = 1$, $R = 3.09$, $S = 0.11$,
$Time = 277$, $CC = 0.16$, $MSE = 4.10$

Fig. 5. *FCM–SIFT* registration results with CT of head on axial, sagittal, and coronal planes. From left to right: reference, target with salt and pepper noise ($\nu = 0.5$), registered, and error images.

images, the registered image, and the error image defined as the difference between the reference and the registered image. We show also the values of the cross correlation (CC), the root mean square error (MSE), the computation time ($Time$), the value of threshold of the α-cut, the horizontal translation (Tx), the vertical translation (Ty), the rotation degree (R), and the scaling factor (S).

In Fig. 4, we report the results of five experiments (T1–T5), using the axial CT of head illustrated in Fig. 2. The target image is obtained by applying the transformations shown in Tab. 2. Fig. 4a shows the dependence of running time of the *FCM–SIFT* technique on the value of α, that is the threshold of the α-cut. Fig. 4b, in turn, shows the dependence of the cross correlation (CC) between reference and registered images obtained using the *FCM–SIFT* technique on the value of α-cut.

To study the noise robustness of our approach to segmentation, we applied the *FCM–SIFT* technique on noisy orthogonal slices in axial, sagittal, and coronal planes, by adding salt and pepper noise (impulse noise) to the target image. This kind of noise is typically observed on advanced medical imaging equipments such as CT, MRI (Magnetic Resonance Imaging) and PET (Positron Emission Tomography). It appears as randomly occurring sparse light and dark disturbances in the image (white and black pixels). Typical sources include flecks of dust inside the camera, or, with digital cameras, faulty CCD (Charge-Coupled Device) image sensors elements.

We compared the results of registration in the presence of salt and pepper noise using our proposed approach *FCM–SIFT*, a modified version of our approach using *KM* instead of *FCM* (*KM–SIFT*), and standard *SIFT*. In our experiments we notice that the *breakdown point*[1] for standard *SIFT* and *KM–SIFT* is a noise density value $\nu = .4$, as those methods cannot detect the correspondence between reference and target images in the presence of a noise density higher than this value, while the breakdown point of *FCM–SIFT* is $\nu = .59$. Fig. 5 shows the of *FCM–SIFT* registration results in the presence of salt and pepper noise ($\nu = .50$). To increase the breakdown point of *FCM–SIFT* we have to increase α; but this is possible until a critical value where the registration results degrade as we may cut off relevant features.

As shown in Fig. 4a, the average registration time in *FCM–SIFT* is about 30 seconds, while the average registration time in standard *SIFT* is about 4 seconds. For speeding up the clustering phase, we have experimented also a dynamic pyramid approach for clustering, applying *FCM* on low resolution images of increasing size. This pyramidal approach to *FCM* can reduce the average registration time to about 10 seconds.

For speed up the clustering phase, we use a dynamic pyramid approach that allow us to operate on reduced images instead of original images, thus reducing clustering and registration times. Then we reconstruct the pyramid and register the original images after calculating the registration parameters from reduced resampled images obtained from scale resolution pyramid.

[1] We use here this term, borrowed from Robust Statistics [8], as the minimum value of noise density that makes the *SIFT* procedure unsuccessfully.

6 Conclusions

Medical image registration procedures allow us to extract complementary information from different modalities, and to accurately compare images from the same modality [4,10].

This paper proposes an approach to medical image registration using a segmentation step segmentation based on Fuzzy C-Means (*FCM*) clustering [1] and Scale Invariant Feature Transform (SIFT) [6] for matching keypoints in segmented regions.

It is worth noting that the quality of *SIFT* results, as for other feature-based methods for registration, is strongly affected by the quality of the previous region segmentation procedure. To obtain robust segmentation, we applied FCM feature vectors including local information invariant to image scaling and rotation, and to change in illumination [2,12,7].

The paper shows also how to reduce the running time of the clustering step following a dynamic pyramid approach applying *FCM* on low resolution images of increasing size. The reported speed-up is about three.

Medical images are often corrupted by noise; in particular, salt and pepper noise is typically observed on advanced medical imaging equipments. The robustness of algorithms with respect to noise is then a major request in medical imaging. From our experimental results, we can conclude that the proposed *FCM–SIFT* registration method is more robust to noise artifacts than standard *SIFT* and a modified version of our approach using *KM* instead of *FCM*.

Acknowledgements

Work partially funded by a grant of the University of Genova. Hassan Mahmoud is a PhD student in Computer Science at DIBRIS, University of Genova.

References

1. J.C. Bezdek. ”Pattern Recognition with Fuzzy Objective Function Algorithms”. Plenum Press, New York, 1981.
2. W. Cai, S. Chen, D. Zhang. ”Fast and robust fuzzy c-means clustering algorithms incorporating local information for image segmentation”, *Pattern Recognition*. 40:825–838, 2007.
3. R.O. Duda, P.E. Hart. ”Pattern Classification and Scene Analysis”. Wiley, New York, 1973.
4. L. Hallpike, D.J. Hawkes. ”Medical image registration: an overview”. *Imaging*, 14:455–463, 2002.
5. S. Lloyd. ”Last square quantization in PCM's.” *Bell Telephone Laboratories Paper*, 1957; also, *IEEE Trans. Inform. Theory*, 28:129–137, 1982.
6. D.G., Lowe. ”Object recognition from local scale-invariant features”. *Proceedings of the International Conference on Computer Vision*, 1150–1157, 1999.
7. J.L. Foo, G. Miyano, T. Lobe, E. Winer,. ”Three-dimensional segmentation of tumors from CT image data using an adaptive fuzzy system”. *Computers in Biology and Medicine*, 62:869–878, 2009.
8. P. J. Huber. ”Robust Statistics”. Wiley, 1981.

9. Z.-X. Ji, Q.-S. Sun, D.-S. Xia. "A modied possibilistic fuzzy c-means clustering algorithm for bias eld estimation and segmentation of brain MR image". *Computerized Medical Imaging and Graphics*, 35:383–397, 2011.
10. J.B.A. Maintz, M.A. Viergever. A survey of Medical Image Registration, *Medical Image Analysis*, 2:1–36, 1988.
11. F. Masulli, A. Schenone. A fuzzy clustering based segmentation system as support to diagnosis in medical imaging. *Artificial Intelligence in Medicine*, 16:129–147, 1999.
12. A. Moreno, C.M. Takemura, O. Colliot, O. Camara, I. Bloch. Using anatomical knowledge expressed as fuzzy constraints to segment the heart in CT images. *Pattern Recognition*, 41:2525–2540, 2008.
13. N. Sharma, A.K. Ray, S. Sharma, K.K. Shukla, S. Pradhan, L.M. Aggarwal. "Segmentation and classification of medical images using texture-primitive features: Application of BAM-type artificial neural network". *J Med Phys*, 33:119–126, 2008.
14. N. Sharma, L.M. Aggarwal. "Automated medical image segmentation techniques". *J Med Phys*, 35:3–14, 2010.
15. H. Steinhaus, H.: Sur la division des corp materiels en parties. Bulletin de l'Academie Polonaise des Sciences, C1. III **IV** (1956) pp. 801–804.